Journal of Applied Mechanics and Technical Physics, Vol. 49, No. 1, pp. 71–79, 2008

WAVE RESISTANCE OF AN AIR-CUSHION VEHICLE IN UNSTEADY MOTION OVER AN ICE SHEET

A. V. Pogorelova

UDC 532.59:629.576

Unsteady rectilinear motion of an air-cushion vehicle over an ice sheet at various speeds is considered. Ice is modeled by a viscoelastic ice plate. The effects of the basin depth, the thickness and relaxation time of ice, vehicle length, acceleration, deceleration, and speed of uniform motion on the wave resistance of the vehicle are analyzed. Maneuvering methods for increasing or lowering the wave resistance of the vehicle are proposed.

Key words: *incompressible liquid, viscoelastic ice plate, air-cushion vehicle, unsteady motion, wave resistance.*

1. The hydrodynamic problem of an air-cushion vehicle (ACV) moving over continuous ice is modeled by a system of surface pressures [1] moving above the floating ice plate [2]. The specified system of surface pressures q moves at a speed $u(t)$ over an infinite region covered by continuous ice. The coordinate system attached to the vehicle is located as follows: the plane xOy coincides with the unperturbed ice–water interface, the x direction coincides with the direction of motion of the vehicle, and the z axis is directed vertically upward. It is assumed that water is an ideal incompressible liquid of density ρ_2 and that the motion of the liquid is potential. Ice cover is modeled by a viscoelastic, initially unstrained, homogeneous, isotropic plate. The period of wave processes in the ice cover is considered to be much smaller than the relaxation time of ice. Following [2], for ice we use the deformation law of a linear retarded elastic Kelvin–Voigt medium [3].

According to [1, 4] the wave resistance acting on the ACV is calculated by the formula

$$R = \iint\limits_{\Omega} q\,\frac{\partial w}{\partial x}\,dx\,dy, \tag{1.1}$$

where Ω is the region of distribution of the load $q(x, y, t)$ and $w(x, y, t)$ is the displacement of the liquid surface or the vertical displacement of ice.

The linearized kinematic condition on the ice–water interface has the form

$$\frac{\partial \Phi}{\partial z}\Big|_{z=0} = \frac{\partial w}{\partial t} - u\,\frac{\partial w}{\partial x}, \tag{1.2}$$

where $\Phi(x, y, z, t)$ is the liquid speed potential function which satisfies the Laplace equation $\Delta\Phi = 0$.

Under the above assumptions, the linearized boundary conditions for w and Φ are written as

$$\begin{gathered}\frac{Gh^3}{3}\Big(1 + \tau_k\,\frac{\partial}{\partial t} - \tau_k u\,\frac{\partial}{\partial x}\Big)\nabla^4 w + \rho_1 h\Big(\frac{\partial^2 w}{\partial t^2} - \dot{u}\,\frac{\partial w}{\partial x} - 2u\,\frac{\partial^2 w}{\partial t\,\partial x} + u^2\,\frac{\partial^2 w}{\partial x^2}\Big) \\ = -\rho_2 g w - \rho_2\Big(\frac{\partial \Phi}{\partial t} - u\frac{\partial \Phi}{\partial x}\Big) - q, \qquad z = 0, \\ \frac{\partial \Phi}{\partial z} = 0, \qquad z = -H.\end{gathered} \tag{1.3}$$

Institute of Machine Science and Metallurgy, Far East Division, Russian Academy of Sciences, Komsomol'sk-on-Amur 681005; sasha@imim.ru. Translated from Prikladnaya Mekhanika i Tekhnicheskaya Fizika, Vol. 49, No. 1, pp. 89–99, January–February, 2008. Original article submitted October 31, 2006; revision submitted January 11, 2007.

Here $G = 0.5E/(1+\nu)$ is the elastic shear modulus of ice, E is Young's module, ν is Poisson's ratio, τ_k is the stress relaxation time of ice or the retardation time [2, 3], $h(x,y)$ is the ice layer thickness, $\rho_1(x,y)$ is the ice density, $H = H_1 - b$, H_1 is the basin depth, and $b = \rho_1 h/\rho_2$ is the ice submergence depth in static equilibrium. For great depths, where H_1 is much larger than h, we can set $H \approx H_1$. Below, it is assumed that the quantities ρ_1 and h are constant. In the calculation, the quantities G and ρ_1 are taken to be their normalized values (the integrated quantities over the plate thickness).

If, at the time $t = 0$, the vehicle does not move and there are no perturbations, except for the static deformation of the ice plate, the initial conditions for the function $\Phi(x,y,z,t)$ are written as

$$\frac{\partial\Phi}{\partial z}\Big|_{\substack{z=0\\t=0}} = 0, \qquad \Big(\frac{\partial\Phi}{\partial t} + \frac{\rho_1 h}{\rho_2}\,\frac{\partial^2\Phi}{\partial z\partial t}\Big)\Big|_{\substack{z=0\\t=0}} = 0. \tag{1.4}$$

It is assumed that the change in the ACV speed with time can be approximately expressed by the formula

$$u = u_1 \tanh\,(\mu_1 t) + (u_2 - u_1)\,\frac{\tanh\,(\mu_2(t-t_2)) + \tanh\,(\mu_2 t_2)}{2}$$

$$+ (u_3 - u_2)\,\frac{\tanh\,(\mu_3(t-t_3)) + \tanh\,(\mu_3 t_3)}{2}, \tag{1.5}$$

where u_1, u_2, and u_3 are the successive values of the vehicle speed; μ_1, μ_2, and μ_3 are coefficients that characterize the acceleration (deceleration) of the vehicle; the values t_2 and t_3 are the times at which the vehicle acceleration is $\mu_2(u_2 - u_1)/2$ and $\mu_3(u_3 - u_2)/2$, respectively, and are the inflection points of the function $u(t)$.

In the present paper, the following modes of change in the vehicle speed (1.5) (modes of motion) with time are investigated:

1) acceleration → motion at a specified speed; 2) acceleration → motion at a specified speed → deceleration to a full stop; 3) acceleration → motion at a first specified speed → acceleration → motion at a second specified speed; 4) acceleration → motion at a first specified speed → deceleration → motion at a second specified speed; 5) acceleration → motion at a specified speed → deceleration to a full stop → acceleration → motion at a specified speed.

According to (1.5), the distance traveled by the vehicle is calculated by the formula

$$s = \frac{u_1}{\mu_1}\,\ln\left(\cosh\,(\mu_1 t)\right) + \frac{u_2 - u_1}{2}\Big(\frac{1}{\mu_2}\ln\Big(\frac{\cosh\,(\mu_2(t-t_2))}{\cosh\,(\mu_2 t_2)}\Big) + \tanh\,(\mu_2 t_2)t\Big)$$

$$+ \frac{u_3 - u_2}{2}\Big(\frac{1}{\mu_3}\,\ln\Big(\frac{\cosh\,(\mu_3(t-t_3))}{\cosh\,(\mu_3 t_3)}\Big) + \tanh\,(\mu_3 t_3)t\Big). \tag{1.6}$$

It is assumed that in the specified moving coordinate system, the pressure $q(x,y)$ does not depend on time. The system of moving pressures is given by a function $q(x,y)$ in the form [5, 6]

$$q(x,y) = q_0[\tanh\,(\alpha_1(x + L/2)) - \tanh\,(\alpha_1(x - L/2))]$$

$$\times\,[\tanh\,(\alpha_2(y + L/(2\omega))) - \tanh\,(\alpha_2(y - L/(2\omega)))]/4, \tag{1.7}$$

where q_0 is the nominal pressure, L is the vehicle length, $\omega = L/B$ is the vehicle aspect ratio, B is the vehicle width, α_1 and α_2 are parameters that characterize the deviation of the pressure distribution in the longitudinal and transverse directions from a rectangular shape. The larger the values of α_1 and α_2, the closer the pressure distribution to a rectangular shape. For $\alpha_1 \to \infty$ and $\alpha_2 \to \infty$, the pressure q is equivalent to the pressure q_0 distributed uniformly over a rectangle.

2. To obtain an analytical solution of the problem, we make the formulation dimensionless. For this, we introduce the characteristic dimension — the vehicle length L — and the characteristic speed u_0, which is taken to be the minimum phase speed for the liquid of infinite depth $u_{\min} = 2(Dg^3/(27\rho_2))^{1/8}$ [2]. Here $D = Eh^3/(12(1-\nu^2))$. We introduce the following dimensionless variables, functions, and parameters:

$$x' = \frac{x}{L}, \quad y' = \frac{y}{L}, \quad z' = \frac{z}{L}, \quad t' = \frac{tu_0}{L}, \quad \tau_k' = \frac{\tau_k u_0}{L}, \quad \Phi' = \frac{\Phi u_0}{gL^2}, \quad w' = \frac{w}{L},$$

$$q' = \frac{q}{\rho_2 gL}, \quad u' = \frac{u}{u_0}, \quad s' = \frac{s}{L}, \quad \mu_i' = \frac{\mu_i L}{u_0}, \quad u_i' = \frac{u_i}{u_0}, \quad i = \overline{1,3}$$

(below, the primes at the dimensionless quantities are omitted). In view of (1.2), boundary condition (1.3) for $z = 0$ can be written in the dimensionless variables as

$$\varkappa k_L\Big(1 + \tau_k \frac{\partial}{\partial t} - \tau_k u \frac{\partial}{\partial x}\Big)\nabla^4 \frac{\partial \Phi}{\partial z} + \varepsilon\Big(\frac{\partial^3 \Phi}{\partial z\, \partial t^2} - \dot{u}\, \frac{\partial^2 \Phi}{\partial z\, \partial x} - 2u\, \frac{\partial^3 \Phi}{\partial t\, \partial x\, \partial z} + u^2\, \frac{\partial^3 \Phi}{\partial x^2\, \partial z}\Big)$$

$$= -k_L\, \frac{\partial \Phi}{\partial z} - \Big(\frac{\partial^2 \Phi}{\partial t^2} - \dot{u}\, \frac{\partial \Phi}{\partial x} - 2u\, \frac{\partial^2 \Phi}{\partial t\, \partial x} + u^2\, \frac{\partial^2 \Phi}{\partial x^2}\Big) - \frac{\partial q}{\partial t} + u\, \frac{\partial q}{\partial x}, \tag{2.1}$$

where $\varkappa = Gh^3/(3\rho_2 g L^4)$, $k_L = gL/u_0^2$, and $\varepsilon = \rho_1 h/(\rho_2 L)$.

In addition, it is assumed that the functions $\Phi(x, y, z, t)$ and $q(x, y)$ satisfy the conditions required to represent them as Fourier integral expansions in the variables x and y. Following [5, 7], we write

$$\Phi(x, y, z, t) = \frac{1}{4\pi^2} \int\limits_0^\infty k\, dk \int\limits_{-\pi}^{\pi} d\theta \iint\limits_\Omega (F \exp(-kz) + E \exp(kz))$$

$$\times \exp(ik((x - x_1)\cos\theta + (y - y_1)\sin\theta))\, dx_1\, dy_1,$$

$$q(x, y) = \frac{1}{4\pi^2} \int\limits_0^\infty k\, dk \int\limits_{-\pi}^{\pi} d\theta \iint\limits_\Omega q(x_1, y_1) \exp(ik((x - x_1)\cos\theta + (y - y_1)\sin\theta))\, dx_1\, dy_1 \tag{2.2}$$

(F and E are unknown functions of the variables x_1, y_1, t, k, and θ).

Substituting expressions (2.2) into boundary condition (2.1) and the dimensionless boundary condition (1.3) for $z = -\gamma$, where $\gamma = H/L$, we obtain the relation between the quantities F and E and the differential equation for F:

$$E = F \exp(2k\gamma); \tag{2.3}$$

$$\ddot{F} - 2\dot{F}u\sigma + Fu^2\sigma^2 - F\dot{u}\sigma + \frac{k_L k \tanh(k\gamma)(F(1 + \varkappa k^4(1 - \tau_k u\sigma)) + \dot{F}\tau_k \varkappa k^4)}{\varepsilon k \tanh(k\gamma) + 1}$$

$$= \frac{uq\sigma}{(1 + \exp(2k\gamma))(\varepsilon k \tanh(k\gamma) + 1)}, \qquad \sigma = ik\cos\theta. \tag{2.4}$$

To solve Eq. (2.4), following [5, 7], we introduce the function

$$F_1 = F \exp(-\sigma s), \tag{2.5}$$

where $s(t) = \int\limits_0^t u(\tau)\, d\tau$ is the dimensionless distance traveled by the ACV in time t.

Substitution of (2.5) into (2.4) yields the equation

$$\ddot{F}_1 + \dot{F}_1 \frac{k_L \varkappa \tau_k k^5 \tanh(k\gamma)}{\varepsilon k \tanh(k\gamma) + 1} + \frac{F_1 k_L k \tanh(k\gamma)(1 + \varkappa k^4)}{\varepsilon k \tanh(k\gamma) + 1} = \frac{u(t) q(x_1, y_1)\sigma \exp(-\sigma s(t))}{(1 + \exp(2k\gamma))(\varepsilon k \tanh(k\gamma) + 1)}.$$

Solving this equation with the use of the Laplace transform, initial conditions (1.4), and the convolution theorem, we have

$$F_1 = \int\limits_0^t f(\tau) K_1 \exp\Big(-\frac{\beta_1}{2}(t - \tau)\Big)\, d\tau, \tag{2.6}$$

where

$$f(\tau) = \frac{u(\tau) q(x_1, y_1)\sigma \exp(-\sigma s(\tau))}{(1 + \exp(2k\gamma))(\varepsilon k \tanh(k\gamma) + 1)}, \qquad K_1 = \begin{cases} \sin(\sqrt{\beta}(t - \tau))/\sqrt{\beta}, & \beta > 0, \\ \sinh(\sqrt{-\beta}\,(t - \tau))/\sqrt{-\beta}, & \beta < 0, \\ t - \tau, & \beta = 0, \end{cases}$$

$$\beta = \beta_2 - \frac{\beta_1^2}{4}, \qquad \beta_1 = \frac{\varkappa\tau_k k_L k^5 \tanh\,(k\gamma)}{\varepsilon k \tanh\,(k\gamma) + 1}, \qquad \beta_2 = \frac{k_L k \tanh\,(k\gamma)(1 + \varkappa k^4)}{\varepsilon k \tanh\,(k\gamma) + 1}.$$

Substituting (2.3) and (2.5) in (2.2), we obtain the following expression for the function Φ:

$$\Phi(x, y, z, t) = \frac{1}{4\pi^2} \int\limits_0^\infty k\,dk \int\limits_{-\pi}^{\pi} d\theta \iint\limits_\Omega F_1 \exp(\sigma s)(\exp(-kz) + \exp(k(z + 2\gamma)))$$

$$\times \exp(ik((x - x_1)\cos\theta + (y - y_1)\sin\theta))\,dx_1\,dy_1. \tag{2.7}$$

To find the wave resistance R from formula (1.1), it is necessary to express the deflection w in terms of the functions Φ and q. For this, we use the boundary condition (1.3) in dimensionless form

$$\varkappa\Big(1 + \tau_k \frac{\partial}{\partial t} - \tau_k u \frac{\partial}{\partial x}\Big)\nabla^4 w + w = \varphi(x, y, t),$$
$$\varphi(x, y, t) = -q - \frac{\partial\Phi}{\partial t}\Big|_{z=0} + u \frac{\partial\Phi}{\partial x}\Big|_{z=0} - \varepsilon \frac{\partial^2\Phi}{\partial z\,\partial t}\Big|_{z=0} + \varepsilon u \frac{\partial^2\Phi}{\partial z\,\partial x}\Big|_{z=0}. \tag{2.8}$$

An asymptotic analysis of Eq. (2.8) as a function of the parameter $\varkappa$ is given below. For the values of $\varkappa \ll 1$ corresponding to a thin ice layer and large vehicle dimensions, the asymptotic solution of Eq. (2.8) is sought in the form

$$w_i = w_i^0 + \varkappa w_i^1 + \dots\ . \tag{2.9}$$

Substitution of (2.9) into (2.8) yields the following values for the functions w_i^0, w_i^1 and w_i:

$$w_i^0 = \varphi(x, y, t), \qquad w_i^1 = -\Big(1 + \tau_k \frac{\partial}{\partial t} - \tau_k u \frac{\partial}{\partial x}\Big)\nabla^4\varphi(x, y, t),$$
$$w_i = \Big(1 - \varkappa\nabla^4 - \varkappa\tau_k \frac{\partial}{\partial t}\nabla^4 + \varkappa\tau_k u \frac{\partial}{\partial x}\nabla^4\Big)\varphi(x, y, t). \tag{2.10}$$

Setting $\tau_k = 0$ in (2.10) (the relaxation time is equal to zero, and the plate is purely elastic) and taking into account the form of the function φ (2.8) and expansions (2.2) and (2.7), we express w_i as follows:

$$w_i(x, y, t) = \frac{1}{4\pi^2} \int\limits_0^\infty k\,dk \int\limits_{-\pi}^{\pi} d\theta \iint\limits_\Omega \varphi(x_1, y_1, t)(1 - \varkappa k^4)$$

$$\times \exp(ik((x - x_1)\cos\theta + (y - y_1)\sin\theta))\,dx_1\,dy_1. \tag{2.11}$$

For large values of $\varkappa$ ($\varkappa \to \infty$) (a thick ice layer and small vehicle dimensions), the asymptotic solution of Eq. (2.8) is sought in the form

$$w_e = w_e^0 + \dots\ ,$$

where w_e^0 is a solution of the equation

$$\Big(1 + \tau_k \frac{\partial}{\partial t} - \tau_k u \frac{\partial}{\partial x}\Big)\nabla^4 w = 0. \tag{2.12}$$

We note that any solution of the equation $\nabla^4 w = 0$ is symmetric about the plane yOz and, hence, the wave resistance R is equal to zero [see formula (1.1)]. It is assumed that, for $\varkappa \to \infty$, a particular solution of Eq. (2.12) is the solution $w_e^0 = 0$. Then, in view of Eq. (2.11), the function w can be expressed as

$$w(x, y, t) = \frac{1}{4\pi^2} \int\limits_0^\infty k\,dk \int\limits_{-\pi}^{\pi} d\theta \iint\limits_\Omega \varphi(x_1, y_1, t) M(\varkappa) \times \exp(ik((x - x_1)\cos\theta + (y - y_1)\sin\theta))\,dx_1\,dy_1, \tag{2.13}$$

where

$$M(\varkappa) \to 1 - k^4\varkappa \qquad (\varkappa \to 0); \tag{2.14}$$

$$M(\varkappa) \to 0 \qquad (\varkappa \to \infty). \tag{2.15}$$

Thus, we have bilateral asymptotic expansions of the function $M(\varkappa)$ for small and large values of $\varkappa$. The interpolation formula for the quantity $M(\varkappa)$ in the region $0 \leqslant \varkappa < \infty$ is constructed by asymptotic interpolation [8, 9]. According to this method, the quantity $M(\varkappa)$ is sought in the form

$$M(\varkappa) = 1 - k^4 \varkappa \Psi(\varkappa), \qquad \Psi(0) = 1. \tag{2.16}$$

For $\varkappa \to 0$, formula (2.16) retains the same order of accuracy as the asymptotic representation (2.14). The function $\Psi(\varkappa)$ is specified *a priori* and depends on several parameters, which are chosen so that the approximate formula (2.16) yields a correct asymptotic representation of specified accuracy for the other limiting case as $\varkappa \to \infty$. In the particular case where only the higher-order term of the asymptotic representation $M(\varkappa)$ is known for $\varkappa \to \infty$, this function is taken to be the function $\Psi(\varkappa) = (1 + C\varkappa^l)^m$ [8, 9]. For $m = -1$, passing to the limit as $\varkappa \to \infty$ and comparing expressions (2.15) and (2.16), we obtain $\Psi(\varkappa) = (1 + k^4\varkappa)^{-1}$ and, hence, $M(\varkappa) = (1 + k^4\varkappa)^{-1}$. Thus, in view of (2.13), the expression for w is written as

$$w(x, y, t) = \frac{1}{4\pi^2} \int\limits_0^\infty k\, dk \int\limits_{-\pi}^{\pi} d\theta \iint\limits_\Omega \varphi(x_1, y_1, t)\, \frac{1}{1 + \varkappa k^4}$$

$$\times \exp\left(ik((x - x_1)\cos\theta + (y - y_1)\sin\theta)\right) dx_1\, dy_1, \tag{2.17}$$

where $\varphi(x_1, y_1, t)$ and $\Phi(x, y, z, t)$ are determined from formulas (2.8) and (2.7), respectively.

Substituting (2.17) into (1.1) in view of (1.7), (2.2), (2.6)–(2.8) and making the change of variables $k = \lambda$ and $k\cos\theta = \alpha$, and performing simple transformations similar to the transformations in [5, 7], we obtain the dimensionless wave-resistance coefficient A in the form

$$A = \frac{\pi^2\omega}{(\alpha_1 L)^2(\alpha_2 L)^2} \int\limits_0^t u(\tau) \int\limits_0^\infty \frac{\exp\left(-\beta_1(t - \tau)/2\right) K\lambda}{1 + \varkappa\lambda^4} \int\limits_0^\lambda \cos\left(\alpha(s(t) - s(\tau))\right)$$

$$\times \frac{\sin^2(\alpha/2)\sin^2(\sqrt{\lambda^2 - \alpha^2}/(2\omega))\alpha^2}{\sinh^2(\pi\alpha/(2\alpha_1 L))\sinh^2(\pi\sqrt{\lambda^2 - \alpha^2}/(2\alpha_2 L))\sqrt{\lambda^2 - \alpha^2}}\, d\alpha\, d\lambda\, d\tau, \tag{2.18}$$

where

$$K = \begin{cases} \cos\left(\sqrt{\beta}\,(t - \tau)\right)(1 - \beta_1 \tan\left(\sqrt{\beta}\,(t - \tau)\right)/(2\sqrt{\beta}\,)), & \beta > 0, \\ \cosh\left(\sqrt{-\beta}\,(t - \tau)\right)(1 - \beta_1 \tanh\left(\sqrt{-\beta}\,(t - \tau)\right)/(2\sqrt{-\beta}\,)), & \beta < 0, \\ 1 - \beta_1/2, & \beta = 0, \end{cases}$$

$$\beta = \beta_2 - \frac{\beta_1^2}{4}, \qquad \beta_1 = \frac{\varkappa\tau_k k_L \lambda^5 \tanh\left(\lambda\gamma\right)}{\varepsilon\lambda\tanh\left(\lambda\gamma\right) + 1}, \qquad \beta_2 = \frac{k_L\lambda\tanh\left(\lambda\gamma\right)(1 + \varkappa\lambda^4)}{\varepsilon\lambda\tanh\left(\lambda\gamma\right) + 1},$$

$$R/P = Aq_0/(\rho_2 g L), \qquad P = q_0 L B;$$

the dimensionless functions $u(\tau)$, $s(t)$, and $s(\tau)$ are calculated by formulas (1.5) and (1.6).

3. Numerical calculations using formula (2.18) were performed for the following parameter values: $\rho_2 = 1000$ kg/m^3, $\rho_1 = 900$ kg/m^3, $E = 5 \cdot 10^9$ N/m^2, $\nu = 1/3$, $\alpha_1 L = \alpha_2 L = 10$, $\omega = 2$, and $\tau_k = 0.69$ sec. The relaxation time τ_k was chosen in accordance with the results of [10, 11].

Figure 1 gives a curve of the dimensionless wave resistance coefficient A versus time t for the first mode of vehicle motion. It is obvious that, after the ACV accelerates and approaches uniform motion, its wave resistance tends with time to some constant values dependent on the speed. In contrast to the results of [12], where ice was modeled by a purely elastic plate, the dependences $A(t)$ do not have an oscillatory nature. From Fig. 1 it follows that the vehicle has the highest wave resistance at speeds equal to $u_{\min}$–$1.4u_{\min}$ (curves 3–5). When the vehicle reaches subcritical speeds ($u_1 < u_{\min}$) after acceleration, its wave resistance is low (curves 1 and 2) but, in contrast to the results of [12], it is not equal to zero, If the vehicle reaches supercritical speeds ($u_1 > 1.4u_{\min}$) after acceleration (curves 6 and 7), the wave resistance first increases, then, without having reached the critical values, begins to decrease, and reaches some constant values, much smaller than the critical values. Let us compare the

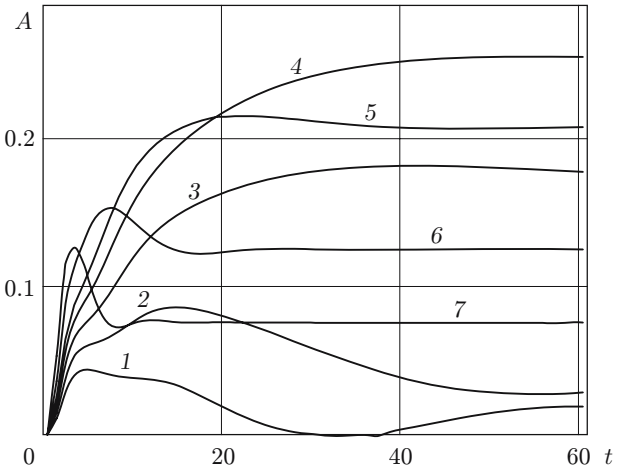

Fig. 1. Wave resistance of ACV versus time for $L = 10$ m, $h = 0.2$ m, $\varepsilon = 0.018$, $\varkappa = 0.038$, $u_{\min} = 8.721$ m/sec, $\tau_k = 0.69$ sec, $\gamma = 4$, and $\mu_1 = 0.5$ sec^{-1}: 1) $u_1 = u_2 = u_3 = 0.6u_{\min}$; 2) $u_1 = u_2 = u_3 = 0.8u_{\min}$; 3) $u_1 = u_2 = u_3 = u_{\min}$; 4) $u_1 = u_2 = u_3 = 1.2u_{\min}$; 5) $u_1 = u_2 = u_3 = 1.4u_{\min}$; 6) $u_1 = u_2 = u_3 = 2u_{\min}$; 7) $u_1 = u_2 = u_3 = 3u_{\min}$.

wave resistance of the vehicle in uniform motion after acceleration and the results obtained for the steady-state problem of vehicle motion over a viscoelastic plate [6].

Figures 2 and 3 show curves of the wave resistance of the vehicle versus speed of motion for thin and thick ice layers, respectively. Curves 1–3 were obtained using formula (2.18) (the unsteady solution) at $t = 100$ in the case of uniform motion at specified speed u_1 after acceleration (the first mode of motion), curves 4–6 are the results of calculations using the formulas from [6] (the steady-state solution of the problem). From Figs. 2 and 3, it follows that the unsteady solution is close to the steady-state one and exceeds it in the case of supercritical speeds ($u > 1.4u_{\min}$); for the critical and subcritical speeds, the difference between the results is larger. Nevertheless, the speeds corresponding to the maximum wave resistance are identical for the steady-state and unsteady solutions: for small and finite depths, the critical speed is close to the value of $\sqrt{gH}$, and for great and infinite depths, it is close to the values of $1.1u_{\min}$–$1.2u_{\min}$. An increase in the ice layer thickness leads to a decrease in the wave resistance. For motion at supercritical speeds, a decrease in the basin depth leads to a certain decrease in the wave resistance at various thickness of the ice layer.

Figure 4 shows the maximum values of the wave resistance A_* at various basin depths γ in the case of uniform motion. Curves 1 and 2 correspond to the unsteady solution [formula (2.18)] and uniform motion of the vehicle after acceleration, and curves 3 and 4 to the steady-state solution of the problem [6]. It is evident that, for the unsteady solution of the problem, the dependence of the maximum wave resistance on depth is nonmonotonic: the maximum wave resistance as a function of the ice layer thickness is in the range $\gamma = 0.5$–1.0. As the depth increases, the wave resistance decreases, and at $\gamma > 1.5$, it reaches a constant value. For very small depths, the unsteady solution also gives smaller values of the wave resistance. A similar effect at a small depth was observed in the experiments of [13]. As the depth decreases in the case of the steady-state solution, the wave resistance increases for a thin ice layer and decreases for a thick ice layer; for small values of γ, the solution diverges. For a thick ice layer and the unsteady mode of motion, the value of γ has little effect on the maximum value of the wave resistance. The difference between the steady-state and unsteady values of the wave resistance for small γ can be attributed to the imperfection of linear wave theory. As is known, linear wave theory is more justified for unsteady solutions of the problem [5].

Figure 5 shows the effects of various modes of acceleration and deceleration on the wave resistance of the ACV. From an analysis of curves 1 and 2, it follows that the higher the initial acceleration of the vehicle in reaching a supercritical speed, the lower the maximum wave resistance of the ACV. This conclusion agrees with the results of [5, 7] for uniformly accelerated motion of ACVs on pure water and in a broken-ice field. Curves 3 and 4 correspond to the wave resistance of the vehicle in reaching a supercritical speed with the subsequent deceleration to a full stop. In this case, the absolute value of the wave resistance is the higher, the smaller the absolute value

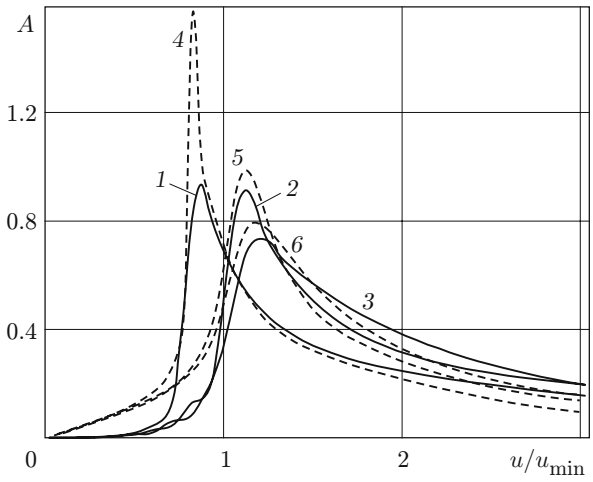

Fig. 2

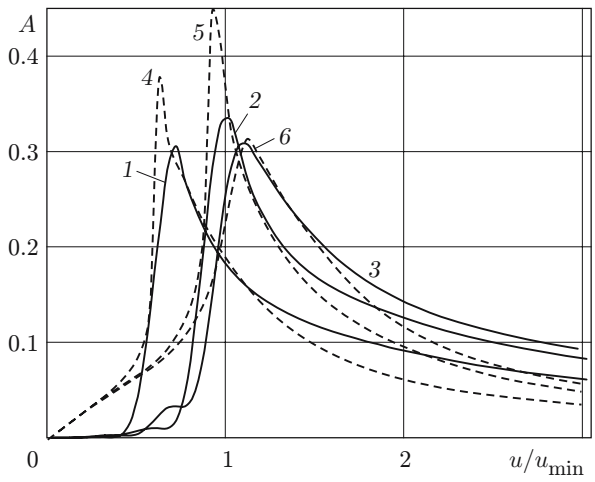

Fig. 3

Fig. 2. Wave resistance of ACV in uniform motion versus speed u for the unsteady solution (1–3) and steady-state solution (4–6) for $L = 10$ m, $h = 0.1$ m, $\varepsilon = 0.009$, $\varkappa = 4.783 \cdot 10^{-3}$, $u_{\min} = 6.725$ m/sec, and $\tau_k = 0.69$ sec: 1) $u_1 = u_2 = u_3 = u$, $\mu_1 = 0.5$ sec^{-1}, $t = 100$ sec, and $\gamma = 0.3$; 2) $u_1 = u_2 = u_3 = u$, $\mu_1 = 0.5$ sec^{-1}, $t = 100$ sec, and $\gamma = 0.7$; 3) $u_1 = u_2 = u_3 = u$, $\mu_1 = 0.5$ sec^{-1}, $t = 100$ sec, and $\gamma = 4$; 4) $\gamma = 0.3$; 5) $\gamma = 0.7$; 6) $\gamma = 4$.

Fig. 3. Wave resistance of ACV in uniform motion versus speed u for the unsteady solution (1–3) and steady-state solution (4–6) for $L = 20$ m, $h = 0.5$ m, $\varepsilon = 0.023$, $\varkappa = 0.037$, $u_{\min} = 12.297$ m/sec, and $\tau_k = 0.69$ sec: 1) $u_1 = u_2 = u_3 = u$, $\mu_1 = 0.5$ sec^{-1}, $t = 100$ sec, and $\gamma = 0.25$; 2) $u_1 = u_2 = u_3 = u$, $\mu_1 = 0.5$ sec^{-1}, $t = 100$ sec, and $\gamma = 0.7$; 3) $u_1 = u_2 = u_3 = u$, $\mu_1 = 0.5$ sec^{-1}, $t = 100$ sec, and $\gamma = 3$; 4) $\gamma = 0.25$; 5) $\gamma = 0.7$; 6) $\gamma = 3$.

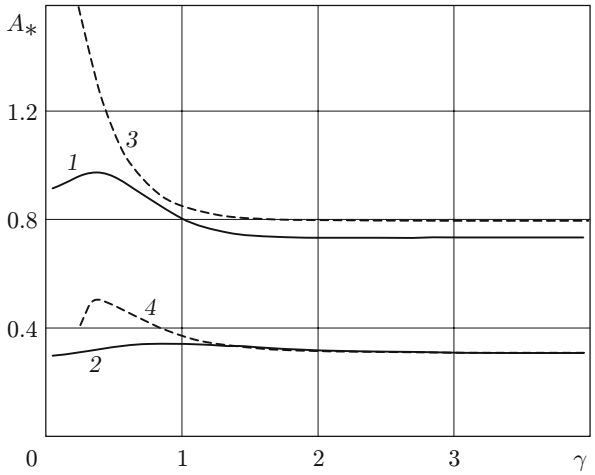

Fig. 4. Maximum wave resistance of the vehicle A_* in uniform motion versus basin depth γ for the unsteady (1 and 2) and steady-state (3 and 4) solutions for $\tau_k = 0.69$ sec: 1) $u_1 = u_2 = u_3 = u$, $\mu_1 = 0.5$ sec^{-1}, $t = 100$ sec, $L = 10$ m, $h = 0.1$ m, $\varepsilon = 0.009$, $\varkappa = 4.783 \cdot 10^{-3}$, and $u_{\min} = 6.725$ m/sec; 2) $u_1 = u_2 = u_3 = u$, $\mu_1 = 0.5$ sec^{-1}, $t = 100$ sec, $L = 20$ m, $h = 0.5$ m, $\varepsilon = 0.023$, $\varkappa = 0.037$, and $u_{\min} = 12.297$ m/sec; 3) $L = 10$ m, $h = 0.1$ m, $\varepsilon = 0.009$, and $\varkappa = 4.783 \cdot 10^{-3}$; 4) $L = 20$ m, $h = 0.5$ m, $\varepsilon = 0.023$, and $\varkappa = 0.037$.

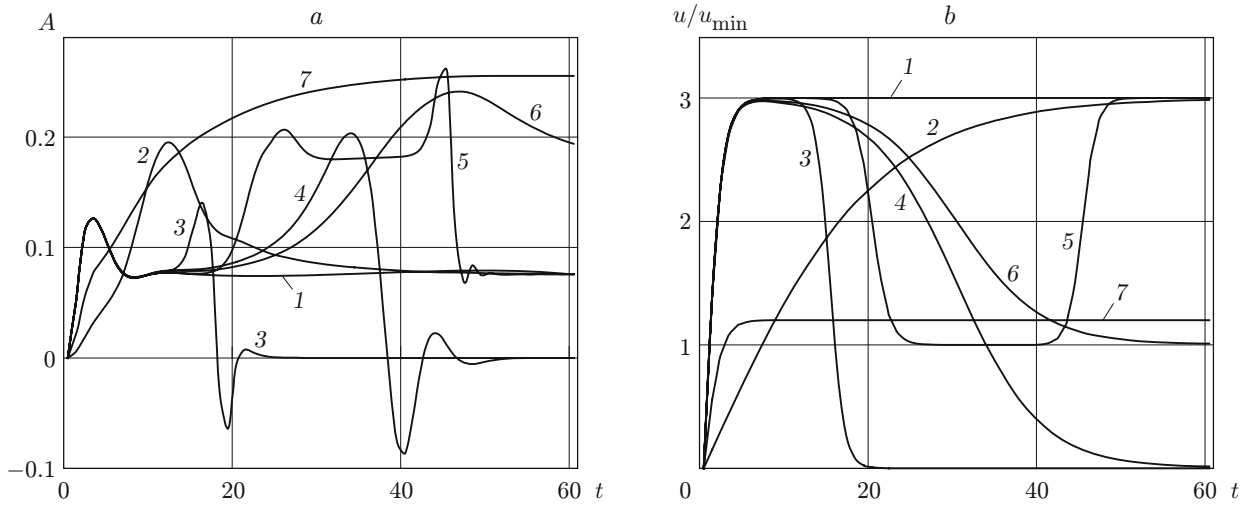

Fig. 5. Wave resistance of ACV (a) and speed of ACV (b) versus time for $L = 10$ m, $h = 0.2$ m, $\varepsilon = 0.018$, $\varkappa = 0.038$, $u_{\min} = 8.721$ m/sec, $\tau_k = 0.69$ sec, and $\gamma = 4$: 1) $u_1 = u_2 = u_3 = 3u_{\min}$ and $\mu_1 = 0.5$ sec^{-1}; 2) $u_1 = u_2 = u_3 = 3u_{\min}$ and $\mu_1 = 0.05$ sec^{-1}; 3) $u_1 = 3u_{\min}$, $u_2 = u_3 = 0$, $\mu_1 = 0.5$ sec^{-1}, $\mu_2 = 0.6$ sec^{-1}, and =15 sec; 4) $u_1 = 3u_{\min}$, $u_2 = u_3 = 0$, $\mu_1 = 0.5$ sec^{-1}, $\mu_2 = 0.1$ sec^{-1}, and $t_2 = 30$ sec; 5) $u_1 = 3u_{\min}$, $u_2 = u_{\min}$, $u_3 = 3u_{\min}$, $\mu_1 = \mu_2 = 0.5$ sec^{-1}, $\mu_3 = 0.6$ sec^{-1}, $t_2 = 20$ sec, and $t_3 = 45$ sec; 6) $u_1 = 3u_{\min}$, $u_2 = u_3 = u_{\min}$, $\mu_1 = 0.5$ sec^{-1}, $\mu_2 = 0.1$ sec^{-1}, and $t_2 = 30$ sec; 7) $u_1 = u_2 = u_3 = 1.2u_{\min}$ and $\mu_1 = 0.5$ sec^{-1}.

of the deceleration coefficient. From an analysis of curve 5, it follows that in the case where the vehicle reaches a supercritical speed, then decelerates to a subcritical speed, and then accelerates to a supercritical speed, the wave resistance also increases. From an analysis of curve 6, it follows that deceleration from a supercritical speed to a subcritical speed with a small deceleration coefficient leads to an increase in the wave resistance. For comparison, Fig. 5 shows curve 7, which is the dependence of the wave resistance on time for acceleration to the critical speed and subsequent motion at the critical speed.

4. The analysis of the results leads to the following conclusions. The ACV has the lowest wave resistance if it moves at subcritical speeds or reaches supercritical speeds at the maximum acceleration and then moves at supercritical speeds. When the ACV moves over ice at supercritical speeds, its deceleration should be performed at the maximum possible absolute deceleration coefficient to prevent the maximum wave resistance and possible ice breakup.

To increase the wave resistance (which is necessary, for example, for resonance breaking of ice sheets by air-cushion vehicles), one can use the following modes of motion:

— attainment of a supercritical speed with the minimum possible acceleration;

— attainment of the critical speed and motion at this speed;

— attainment of a subcritical speed followed by deceleration to a full stop or to the subcritical speed with the subsequent attainment of the supercritical speed;

— attainment of a supercritical speed with the subsequent deceleration to a full stop with the least absolute value of the deceleration coefficient.

Use of asymptotic interpolation to obtain formula (2.18) for the plate deflection w gives good agreement to the well-known steady-state solution for various values of the ice layer thickness, vehicle length, basin depth, and vehicle speed. Nevertheless, it should be noted that the comparison was made for small values of $\varkappa = Gh^3/(3\rho_2 g L^4)$. However, from the experimental results of [14], it follows that ice breaking by the resonance method occurs only for $\varkappa < 0.025$. In the case of large values of $\varkappa$ (great thickness of the layer and small length of the vehicle), the dimensionless wave resistance coefficient of the vehicle A is very small and the wave deflection is insufficiently large to break the ice cover. For example, as was shown in [12] for the steady-state and unsteady solutions, an increase in the ice layer thickness from 0.1 to 0.5 m leads to a factor of 20 decrease in the wave resistance of a vehicle of length $L = 10$ m, with the remaining parameters of the vehicle, basin, and ice being the same (in this case, the value of $\varkappa$ changes from 0.005 to 0.598).

In contrast to the results of [12], if the viscous properties of the ice plate are taken into account, then, first, when entering the mode of uniform motion, the wave resistance of the vehicle does not have an oscillatory nature, and, second, the vehicle moving at subcritical speeds has a small but nonzero wave resistance.

This work was supported by the program "Development of the Scientific Potential of the Higher School (2006–2008)" (Grant No. RNP.2.1.2.1809).

REFERENCES

1. Yu. Yu. Benua, V. K. D'yachenko, B. A. Kolyzaev, et al., *Foundations of the Theory of Air-Cushion Vehicles* [in Russian], Sudostroenie, Leningrad (1970).
2. D. E. Kheisin, *Dynamics of Ice Cover* [in Russian], Gidrometeoizdat, Leningrad (1967).
3. A. M. Freudental and H. Geiringer, *The Mathematical Theories of the Inelastic Continuum*, Springer-Verlag, Berlin (1962).
4. V. P. Bol'shakov, "Wave resistance of the system of surface pressures," in: *Proc. 13th Sci.-Technical Conf. on Ship Theory of the Scientific-Research Society of the Shipbuilding Industry* (Leningrad, September 10–15, 1963), Issue 49, Izd. Tsentr. Nauch-Issled. Inst. Krylova (1963), pp. 68–88.
5. L. J. Doctors and S. D. Sharma, "The wave resistance of an aircushion vehicle in steady and acceleration motion," *J. Ship Res.*, **16**, No. 4, 248–260 (1972).
6. V. M. Kozin and A. V. Pogorelova, "Wave resistance of amphibian aircushion vehicles during motion on ice fields," *J. Appl. Mech. Tech Phys.*, **44**, No. 2, 193–197 (2003).
7. V. M. Kozin and A. V. Pogorelova, "Effect of broken ice on the wave resistance of an amphibian air-cushion vehicle in nonstationary motion," *J. Appl. Mech. Tech. Phys.*, **40**, No. 6, 1036–1041 (1999).
8. A. D. Polyanin and V. V. Dil'man, "Asymptotic interpolation in problems of mass and heat transfer and hydrodynamics," *Theor. Osn. Khim. Tekhnol.*, **19**, No. 1, 3–11 (1985).
9. A. D. Polyanin and V. V. Dil'man, "New methods of the mass and heat transfer theory. 2. The methods of asymptotic interpolation and extrapolation," *Int. J. Heat Mass Transfer*, **28**, No. 1, 45–58 (1985).
10. V. A. Squire, R. J. Hosking, A. D. Kerr, and P. J. Langhorne, *Moving Loads on Ice Plates*, Kluwer Acad., Dordrecht (1996).
11. T. Takizava, "Deflection of a floating sea ice sheet induced by a moving load," *Cold Regions Sci. Technol.*, **11**, 171–180 (1985).
12. V. M. Kozin and A. V. Pogorelova, "Nonstationary motion of an amphibian air-cushion vehicle on ice fields," in: *Proc. of the 7th ISOPE PACOMS* (Dalian, China, Sept. 17–21, 2006) [Electron. resource], Int. Soc. Offshore Polar Eng., Cupertino (2006), pp. 81–86.
13. V. M. Kozin, A. V. Milovanova, and A. V. Onishchuk, "Experimental and theoretical study of ACV motion in a broken-ice field," in: *Applied Problems of the Mechanics of a Deformable Solid Body and Progressive Technologies in Mechanical Engineering* [in Russian] (collected scientific paper) [in Russian], Dal'nauka, Vladivostok (1997), pp. 120–129.
14. V. M. Kozin, " Resonance method of breaking ice sheets," Doct. Dissertation in Tech. Sci., Vladivostok (1993).